



iMScope QT

Imaging Mass Microscope

Unrivaled Mass Spectrometry Imaging Platform

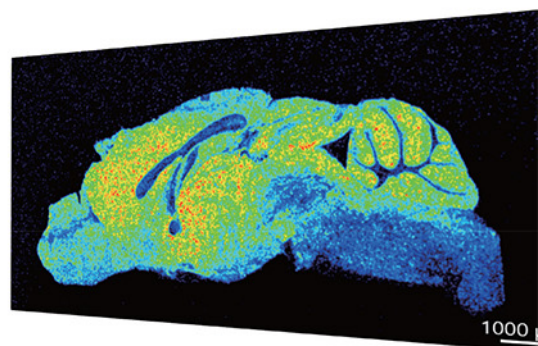
With unparalleled speed, sensitivity and spatial resolution, Shimadzu's **iMScope QT imaging mass microscope** clears the way to next-generation mass spectrometry imaging.

- Fast acquisition of high-mass, high-resolution images at the optical and molecular level
- Simultaneously visualize and analyze samples
- Full fusion with morphology studies
- Integration with the Q-TOF LCMS-9030 enables obtaining distribution information and quantitative data for comprehensive analysis
- Easy switching between MS imaging configuration and LCMS

Learn more about Shimadzu's iMScope QT.








Visit us online at www.ssi.shimadzu.com

Shimadzu Scientific Instruments Inc., 7102 Riverwood Dr., Columbia, MD 21046, USA



RESEARCH ARTICLE

Geocator-tracking seabird migration and moult reveal large-scale, temperature-driven isoscapes in the NE Atlantic

Kelly Atkins¹ | Stuart Bearhop¹  | Thomas W. Bodey²  | W. James Grecian³  |
 Keith Hamer⁴  | Jorge M. Pereira⁵ | Hannah Meinertzhagen¹ | Chris Mitchell¹ |
 Greg Morgan⁶ | Lisa Morgan⁶ | Jason Newton⁷  | Richard B. Sherley¹  |
 Stephen C. Votier⁸ 

¹Centre for Ecology and Conservation, University of Exeter, Cornwall, UK

²School of Biological Sciences, University of Aberdeen, Aberdeen, UK

³Department of Geography, Durham University, Durham, UK

⁴School of Biology, University of Leeds, Leeds, UK

⁵MARE – Marine and Environmental Sciences Centre/ARNET – Aquatic Research Network, Department of Life Sciences, University of Coimbra, Coimbra, Portugal

⁶RSPB Ramsey Island, St Davids, UK

⁷Natural Environment Research Council Life Sciences Mass Spectrometry Facility, Scottish Universities Environmental Research Centre, East Kilbride, UK

⁸Lyell Centre, Institute for Life and Earth Sciences, Heriot-Watt University, Edinburgh, UK

Correspondence

S. C. Votier, Lyell Centre, Institute for Life and Earth Sciences, Heriot-Watt University, Edinburgh, EH14 4AS, UK.
 Email: s.votier@hw.ac.uk

Rationale: By combining precision satellite-tracking with blood sampling, seabirds can be used to validate marine carbon and nitrogen isoscapes, but it is unclear whether a comparable approach using low-precision light-level geolocators (GLS) and feather sampling can be similarly effective.

Methods: Here we used GLS to identify wintering areas of northern gannets (*Morus bassanus*) and sampled winter grown feathers (confirmed from image analysis of non-breeding birds) to test for spatial gradients in $\delta^{13}\text{C}$ and $\delta^{15}\text{N}$ in the NE Atlantic.

Results: By matching winter-grown feathers with the non-breeding location of tracked birds we found latitudinal gradients in $\delta^{13}\text{C}$ and $\delta^{15}\text{N}$ in neritic waters. Moreover, isotopic patterns were best explained by sea surface temperature. Similar isotope gradients were found in fish muscle sampled at local ports.

Conclusions: Our study reveals the potential of using seabird GLS and feathers to reconstruct large-scale isotopic patterns.

1 | INTRODUCTION

Tracking has revolutionised our understanding of animal migration, foraging, and habitat use, but our inference may be limited by sample sizes.^{1–4} Stable isotopes can complement tracking studies but work most effectively when variation in isotopic baselines is independently verified.^{5–7}

In the marine environment, large-scale isotopic gradients (isoscapes), particularly in carbon and nitrogen, highlight the potential for using these markers to infer animal movement or enrich tracking

data.^{8–10} Isoscapes have been constructed utilising particulate organic matter across ocean basins,¹¹ or from other organisms close to the base of the food web, with the potential to trace marine animal movements.¹² An alternative approach is to measure isotopes in the tissues of tracked marine vertebrates. For example, precision satellite-tracking and blood sampling of breeding albatrosses, petrels, and penguins has been used to elucidate regional and latitudinal isoscapes in the Southern Ocean.^{9,13} However, it is unclear whether this approach works during non-breeding when tracking primarily relies upon low-precision (± 200 km) light-level geolocators (GLS¹⁴), and

This is an open access article under the terms of the [Creative Commons Attribution](https://creativecommons.org/licenses/by/4.0/) License, which permits use, distribution and reproduction in any medium, provided the original work is properly cited.

© 2023 The Authors. *Rapid Communications in Mass Spectrometry* published by John Wiley & Sons Ltd.

tissues such as feathers – which tend to be used to represent this period – require information on moult chronology to be applied effectively.¹⁵

Here we measure nitrogen and carbon isotopes in the feathers of non-breeding northern gannets (*Morus bassanus*; hereafter “gannets”) – a partially migratory marine predator with a generally coastal distribution^{16–19} – tracked with GLS to characterise latitudinal isoscapes in the NE Atlantic. We combine feather isotopes with analysis of primary feather moult timing estimated from digital images, and measure isotopes in potential fish prey from the main wintering areas. Our objectives are to (a) determine how isotopes of winter-grown feathers vary spatially in neritic waters in the NE Atlantic, (b) test how $\delta^{13}\text{C}$ and $\delta^{15}\text{N}$ values covary with latitude and sea surface temperature (SST) in feathers and fish, and (c) establish the efficacy of using feather isotopes of GLS -tracked seabirds to construct marine isoscapes.

2 | MATERIAL AND METHODS

2.1 | Study sites and device deployment

Gannets were tracked from three large colonies in the UK and Ireland: Grassholm, Wales (51° 43' N, 05° 28' W); Bass Rock, Scotland (56° 06' N, 02° 36' W); and Great Saltee, Ireland (52° 07' N, 06° 36' W). During July and August 2009–12 or 2018, breeders were captured on their nest using a metal crook or noose attached to a carbon fibre pole (under licence from Natural Resources Wales and Nature Scot) and a GLS logger (either Migrate Technology C330 Mode 6B; British Antarctic Survey MK5, MK15, and MK19) attached using cable ties and superglue either to an acrylic or to a metal leg ring (under licence from the British Trust for Ornithology and their Special Methods Panel). Geolocators did not exceed 0.4% of gannet body mass. Gannets are highly philopatric to nest sites,²⁰ and individuals were recaptured in subsequent years to retrieve geolocators. Birds were sexed genetically from blood samples using 2550F, 2718R or 2757R primers^{21,22} following Stauss et al.²³ We also took a small sample (c. 2–3 cm of the vein) from the distal portion of each tracked birds' primary feather sample (under licence from the UK Home Office) for stable isotopes (see below).

2.2 | Feather moult phenology

Because stable isotopes represent diet during the period of tissue growth, information on feather moult timing is essential for their effective ecological application. Therefore, we analysed moult using 375 dated digital flight images of adult gannets across the NE Atlantic following online searches and social media requests. Photos covered all months of the year and were taken from 2005–2019. Moult scores derived from digital images of seabirds have been shown to be reliable versus scoring moult directly from birds in the field.²⁴ Following filtering for image quality (e.g., where primary feathers were

not clearly visible) and age (split into adult, immature and juvenile based on plumage characteristics²⁰) this provided 313 images enabling two observers to independently quantify adult primary moult on a four-point scale following Meier et al.²⁵ where 0 = an old feather, 1 = a missing feather, 2 = a re-growing feather, 3 = a new fully grown feather. Primary feathers were numbered ascendingly from the innermost (P1 to P10²⁶). Where possible, both wings were scored, but only one was selected at random for inclusion.

Total primary moult scores were rescaled between 0 and 1 and modelled using Underhill & Zucchini²⁷ type one models specified using the R package “moult”²⁸ to estimate mean start date, standard deviation of start date, and mean duration of moult. Scores of each primary feather were also binned by month to visualise the proportion of feathers in each score category. Based on the percentage of feathers in regrowth within the core December wintering period, P8 was chosen for use in stable isotope analysis. Whereas several candidate feathers exhibited regrowth during this period, P8 is also consistent with past studies using SIA in gannet primary feathers,²⁹ allowing us to expand our data set.

2.3 | Geolocation analysis and migratory behaviour

GLS light data were processed, and winter locations calculated for 74 gannets using one of two methods. Birds from Grassholm, Bass Rock, and Great Saltee received British Antarctic Survey MK5, MK15 or MK 19 geolocators during 2009–12, and data were processed as described in Grecian et al.²⁹ Gannets from Grassholm in 2018 received Migrate Technology C330 Mode 6B devices, with timing of sunrise and sunset estimated using a light intensity threshold of 2.5 in TwGeos³⁰ and then position estimated using “FLightR”.³¹ Both methods yielded twice daily location estimates with an accuracy of approximately 200 km.¹⁴ We considered individuals' core wintering areas as the mean of all December locations.^{17,29}

2.4 | Feather sampling

Upon recapture of tracked birds, we cut a 2 × 2 cm notch approximately one third from the distal point of the 8th primary, which were stored in plastic bags prior to analysis. Just prior to stable isotope analysis, feathers were washed thrice with distilled water and placed in a drying oven at 40°C (2010–2012) and 60°C (2019) for 12 h. The feather barbules were then homogenised by cutting into very fine pieces, and a subsample of 0.7 ± 0.1 mg of each weighed into tin cups for stable isotope analysis.

2.5 | Prey fish sampling

Potential gannet prey was collected from five small artisan fish markets during February 2019 along the coast of their wintering areas: Figueira da Foz, Portugal (40° 9' N, 8° 51' W); Tangier (35°

45° N, 5° 50' W); Casablanca (33° 34' N, 7° 35' W); Essaouira (31° 30' N, 9° 45' W), Morocco; and Dakhla, Western Sahara (23° 42' N, 15° 56' W). These markets are dominated by small boats with limited ranges and therefore most likely represent localised catch. Where possible this was verified by talking to the local fishers or fish-sellers on site.

We have no information on gannet diet during non-breeding, so instead we considered a range of functional groups that relate broadly to breeding season prey.³² Each fish was measured and identified to species, then classified by functional group and size class (large pelagic >17.5 cm, small pelagic <17.5 cm, large demersal >17.5 cm, small demersal <17.5 cm). A 1–2 cm³ sample of dorsal muscle tissue was removed and placed in a food dehydrator before being dried at 60°C for 10–12 h, then vacuum sealed in plastic pouches for storage and transport. Dried samples were stored in a –20°C freezer before being lipid-extracted and freeze-dried for 24 h then homogenised to a fine powder using a mortar and pestle.

2.6 | Stable isotope analysis

Stable isotope ratios are reported in δ notation, expressed as parts per thousand (‰) deviation according to the equation $\delta X = [(R_{\text{sample}}/R_{\text{standard}}) - 1] \times 1000$, where X is ¹³C or ¹⁵N, R is the corresponding ratio ¹³C/¹²C or ¹⁵N/¹⁴N, and R_{standard} is the ratio of the international references VPDB for carbon and AIR for nitrogen. Fish muscle and feather subsamples for birds tracked in 2018 were analysed using a Sercon Integra 2 continuous flow stable isotope analyser (Environment & Sustainability Institute, University of Exeter, Exeter, UK). Samples were run alongside in-house reference material (bovine liver; $\delta^{13}\text{C} = -28.61\text{‰} \pm 0.1\text{‰}$, $\delta^{15}\text{N} = 6.32\text{‰} \pm 0.1\text{‰}$ and alanine; $\delta^{13}\text{C} = -19.62\text{‰} \pm 0.1\text{‰}$, $\delta^{15}\text{N} = 1.85\text{‰} \pm 0.1\text{‰}$) to correct for instrument drift. In all cases the standard deviation of the calibration standards was $\pm 0.2\text{‰}$ or lower for $\delta^{15}\text{N}$, and $\pm 0.08\text{‰}$ or lower for $\delta^{13}\text{C}$.

Feather samples from 2009 to 2012 were analysed at the East Kilbride Node of the Natural Environment Research Council Life Sciences Mass Spectrometry Facility (now the National Environmental Isotope Facility) via continuous flow isotope ratio mass spectrometry, using a Thermo Fisher Scientific Delta V Plus interfaced with a Costech ECS 4010 elemental analyser. In-house laboratory standards of GEL (gelatine; $\delta^{13}\text{C} = -20.40\text{‰}$, $\delta^{15}\text{N} = 5.91\text{‰}$), ALA (¹³C-spiked alanine; $\delta^{13}\text{C} = -10.69\text{‰}$, $\delta^{15}\text{N} = 5.91\text{‰}$), GLY (¹⁵N-spiked glycine; $\delta^{13}\text{C} = -36.01\text{‰}$, $\delta^{15}\text{N} = 19.71\text{‰}$) were analysed between every 10 feather samples in the [isotope ratio mass spectrometry](#) (IRMS). Standard deviation of multiple analyses of GELs of different masses in each experimental run was better than $\pm 0.1\text{‰}$ for $\delta^{13}\text{C}$ and $\pm 0.2\text{‰}$ for $\delta^{15}\text{N}$.

In both laboratories, these in-house standards are routinely and regularly checked against international standards such as IAEA-N-1, IAEA-N-2, IAEA-CH-6, USGS 25, USGS 40, and USGS 41, and consequently results from both laboratories are anchored to the V-PDB and AIR scales for $\delta^{13}\text{C}$ and $\delta^{15}\text{N}$, and thus readily comparable.

2.7 | Environmental data

December monthly average or winter seasonal average SST, particulate organic carbon, and chlorophyll a were obtained via the NASA/GFSC Ocean Biology Processing Group (<https://oceancolor.gsfc.nasa.gov/>). Values recorded at 4 km resolution by the MODIS Aqua satellite, as well as depth (global bathymetric data from GEBCO 2020 grid; GEBCO Compilation Group [2021]) were extracted for each gannet December centroid.

2.8 | Statistical analysis

$\delta^{13}\text{C}$ and $\delta^{15}\text{N}$ values of winter-grown feathers were modelled using generalised additive models (GAM; with restricted maximum likelihood) to test the effect of the following conditions at the December centroid: latitude, chlorophyll a, depth, year, colony, and sex. Smoothed terms in the GAMs were subject to double penalisation, which forces the effect size (as effective degrees of freedom) of non-important variables to reduce to near-zero values.³³ GAMs were specified using the “mgcv” package (v 1.8–38³⁴) for R (v. 3.6.1³⁵).

We did not include longitude in our analysis because gannets' neritic habitat use means that variation in carbon and nitrogen isotopes would largely represent inshore/offshore gradients. Similarly, because latitude and SST are highly correlated (Figure S1 [supporting information]), SST was initially excluded, with latitude acting as a proxy for SST. SST was then substituted for latitude in later models to verify performance. A secondary check for variable importance was performed using random forest models,^{36,37} which can cope well with highly collinear data. Results of this secondary random forest analysis (Figure S2 [supporting information]) were used solely as a check on GAM selection and performance.

2.8.1 | GLMM for prey fish

The $\delta^{13}\text{C}$ and $\delta^{15}\text{N}$ values derived from fish muscle were modelled using generalised linear mixed effects models (GLMMs), with latitude as a fixed effect and port as a random effect (because all regional samples were purchased at a single fish market in each port location). Models with and without the fixed effect were compared using χ^2 tests. Standard model check plots and metrics were evaluated to verify model performance was within acceptable parameters. GLMMs were executed using the “lme4” R package³⁸ for R (v. 3.6.1³⁵).

2.8.2 | Modelling isoscapes

$\delta^{13}\text{C}$ and $\delta^{15}\text{N}$ isoscapes were derived by interpolating feather isotopes from gannet centroids via empirical Bayesian kriging (EBK) in ESRI ArcMap 10.5.1. Interpolation was constrained by large marine ecosystem (LME) boundaries,³⁹ which suitably encompassed the main shelf-sea habitat utilised by gannets.

3 | RESULTS

3.1 | Feather moult

Models estimated gannet primary moult commenced by 28 September (± 33.97 days) and lasted (mean \pm SE) 137.2 ± 6.1 days (Table S1 [supporting information]; Figure 1). Adult gannets exhibited two centres of moult and are not necessarily uniform in the starting

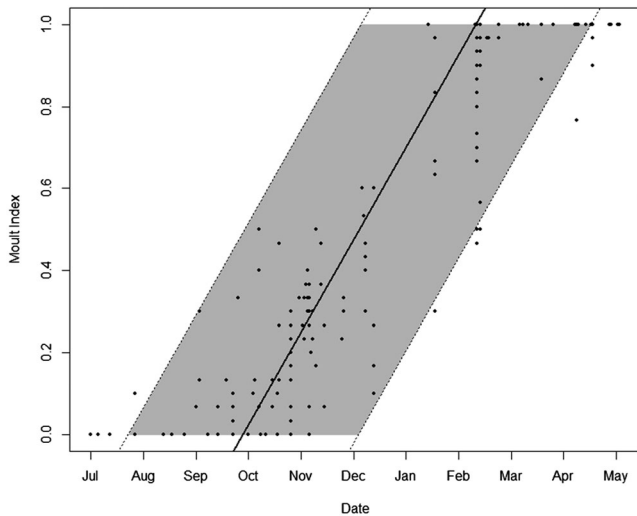


FIGURE 1 Gannet primary moult. Points are values from $n = 313$ adults, the solid line is the mean moult trajectory and the shaded area represents the 95% confidence interval estimated using type 1 models from Underhill and Zucchini (1987) and the R package “moult” (Erni et al 2013)

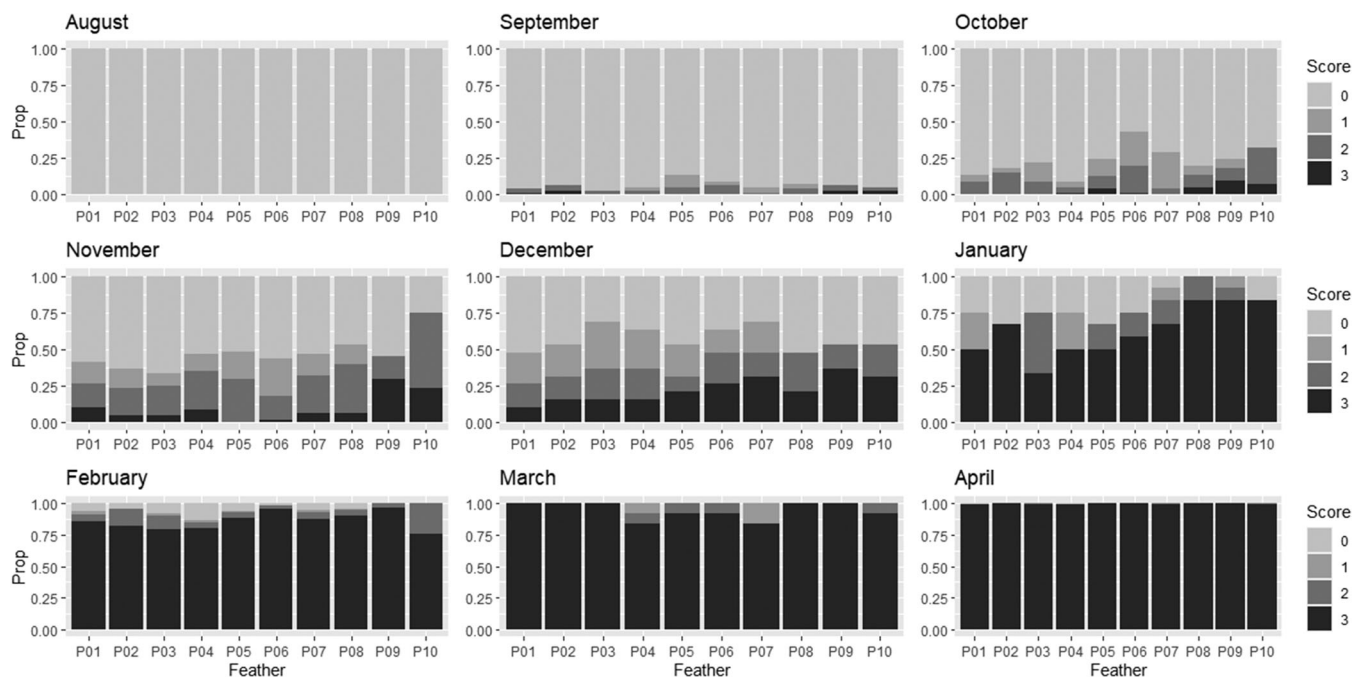


FIGURE 2 Gannet primary moult progression by feather and month ($n = 313$ individuals). Birds are generally in moult during December, which is also the peak timing of non-breeding residency. 0 = old feather, 1 = missing feather, 2 = regrowing feather, 3 = new fully regrown feather

position. Thus, at the population level, our data suggest that most primary feathers are grown during November to January. P8 had the highest proportion of newly regrown feathers between December and January (the core over winter period) and was therefore selected for isotope analysis (Figure 2).

3.2 | Stable isotopes in gannet feathers

$\delta^{13}\text{C}$ values ranged from -16.82‰ to -13.17‰ (mean: -15.12‰). There was a significant negative non-linear effect of latitude on $\delta^{13}\text{C}$ (GAM, $F = 3.87$, $P < 0.001$, Figure 3A), but no effect of year, sex, chlorophyll a or depth (GAM, $P > 0.05$, Figure S3 [supporting information]). Substituting SST for latitude at winter centroids revealed that SST had a significant effect on $\delta^{13}\text{C}$ values (GAM, $F = 3.20$, $P < 0.001$, Figure 3C).

$\delta^{15}\text{N}$ values ranged from 11.96‰ to 18.60‰ (mean: 14.32‰). There was a significant positive non-linear effect of latitude on $\delta^{15}\text{N}$ (GAM, $F = 3.35$, $P < 0.001$, Figure 3B) but no effect of year, sex, chlorophyll a or depth (GAM, $P > 0.05$, Figure S3 [supporting information]). Substituting SST for latitude at winter centroids revealed that SST had a significant effect on $\delta^{15}\text{N}$ (GAM, $F = 3.94$, $P < 0.001$, Figure 3D).

3.3 | Stable isotopes in fish

$\delta^{13}\text{C}$ values from fish muscle ranged from -20.28‰ to -14.84‰ (mean: -18.33‰ , $n = 100$ individuals) and $\delta^{15}\text{N}$ from 7.96‰ to

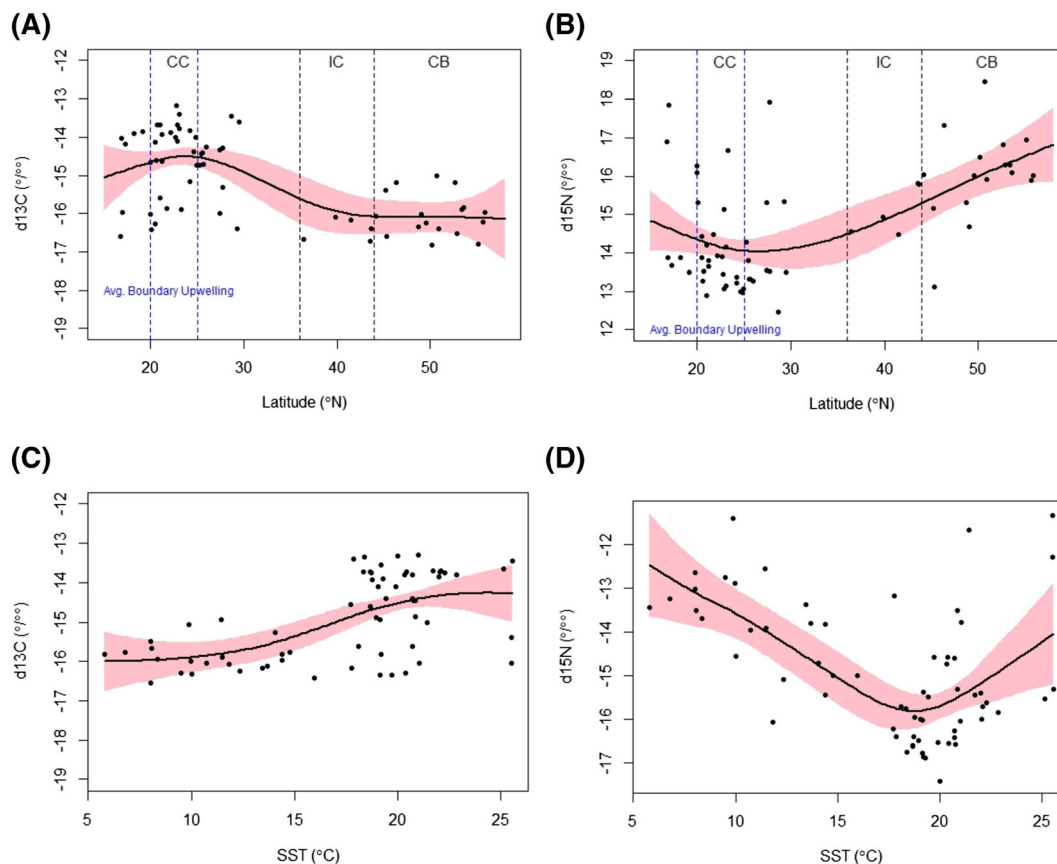


FIGURE 3 Generalised additive model (GAM) results showing significant non-linear relationships between (A), $\delta^{13}\text{C}$ and latitude; (B), $\delta^{15}\text{N}$ and latitude; (C), $\delta^{13}\text{C}$ and sea surface temperature (SST) $^{\circ}\text{C}$; (D), $\delta^{15}\text{N}$ and SST. The solid line is the model estimated mean, and the pink polygon represents the model standard error. For each section vertical blue dashed lines indicate the average latitudinal boundaries of the coastal upwelling plume in the Canary Current large marine ecosystem (LME). Latitudinal LME boundaries for the complete study area are indicated by vertical black dashed lines on plots A and B. CC = Canary Current LME, IC = Iberian coastal LME, CB = Celtic-Biscay shelf LME [Color figure can be viewed at wileyonlinelibrary.com]

12.83‰ (mean: 10.98‰). $\delta^{13}\text{C}$ values were negatively correlated with latitude (GLM; $\chi^2_1 = 5.98$, $P < 0.05$, Figure 4), but this was not the case for $\delta^{15}\text{N}$ values ($\chi^2_1 = 1.30$, $P = 0.25$, Figure 4).

3.4 | Gannet non-breeding distribution and isoscapes

Of 74 tracked birds, 49 (66.2%) wintered in the Canary Current LME, 6 (8.1%) in the Iberian Coastal LME, 12 (16.2%) in the Celtic Biscay Shelf LME, 6 (8.1%) in the North Sea LME, and 1 (1.4%) in the Mediterranean (Figure 5).

Isoscapes interpolated from gannet winter centroids and $\delta^{13}\text{C}$ values of their feathers showed a strong latitudinal gradient, but this was best explained by SST, likely because of cooler upwelling in the Canary Current LME (CCLME; between approximately 20°N and 25°N , off Western Sahara and Mauritania; Figure 5A). Similarly, $\delta^{15}\text{N}$ values of winter grown gannet feathers showed a positive south to north gradient with their winter location from GLS (Figure 5B).

4 | DISCUSSION

Here we measured carbon and nitrogen isotopes of winter-grown gannet feathers by matching individual feathers with GLS-derived non-breeding locations and found spatial isotopic differences (Figure 5). In particular, isotopes varied latitudinally in NE Atlantic neritic waters, most likely due to differences in SST (Figure 3). We discuss this finding and the potential application of tracking marine predators with GLS to inform spatial isotopic patterns.

As in previous studies,¹³ we show that $\delta^{13}\text{C}$ is negatively correlated with latitude and positively with SST, most likely because of less rapid turn-over of heavier carbon isotopes in photosynthetic reactions at colder temperatures.⁵ This is exemplified by the non-linear patterns between 20°N and 25°N , which is associated with the Canary Current cold-water upwelling plume (Figure 3). We also found a positive latitudinal gradient in $\delta^{15}\text{N}$, which may be a result of higher anthropogenic nutrient input in northern European waters.¹⁰

We used EBK to interpolate isotope variation between gannet locations and up to the edges of respective LMEs to produce isoscape models (Figure 5). This approach generates uncertainty in areas with

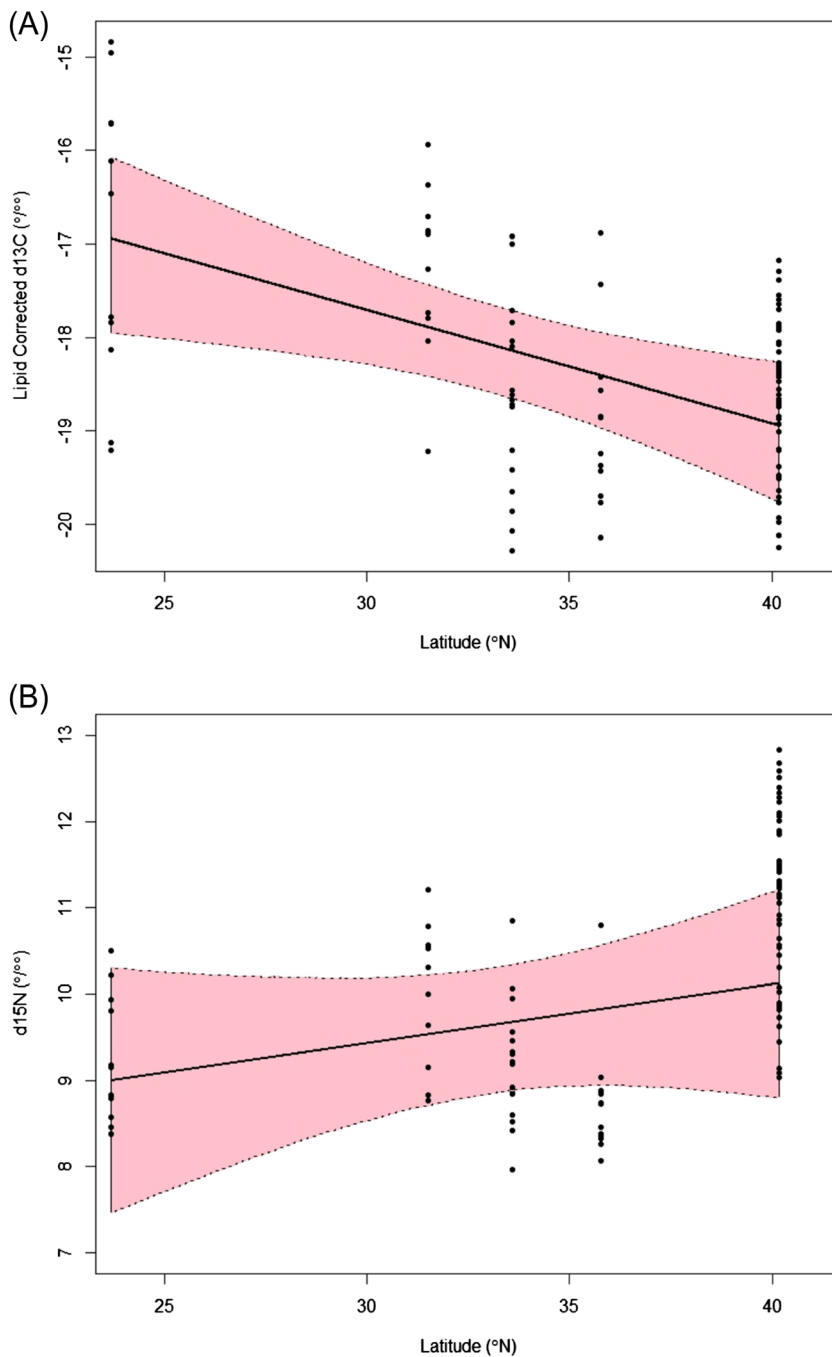


FIGURE 4 (A), Lipid-corrected $\delta^{13}\text{C}$ and (B), $\delta^{15}\text{N}$ values of pelagic fish covary with latitude across northern gannet wintering range. Samples from artisan fish markets in Figueira da Foz, Portugal; Tangier, Morocco; Casablanca, Morocco; Essaouira, Morocco; and Dakhla, Western Sahara. Solid lines are estimates from generalised linear mixed effects models with port fitted as a random effect. The pink-shaded polygon shows the bootstrapped 95% confidence interval [Color figure can be viewed at [wileyonlinelibrary.com](https://onlinelibrary.wiley.com/doi/10.1002/rcm.9489)]

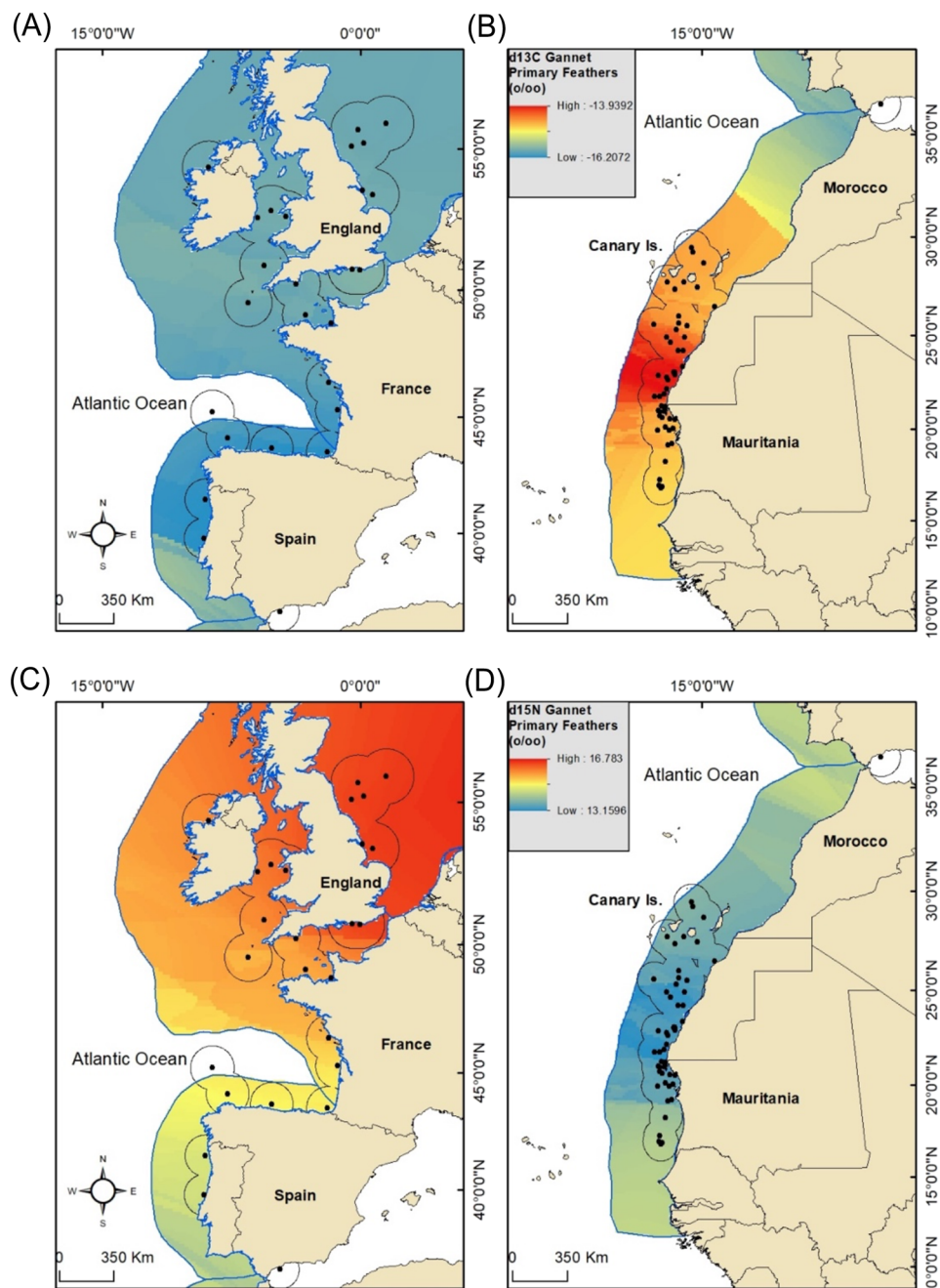
few or no gannet locations, and therefore our findings should be viewed primarily as proof of concept for using geolocator-tracked seabirds to generate marine isoscapes. A comparison with other approaches reveals that $\delta^{15}\text{N}$ and $\delta^{13}\text{C}$ variation shown here (Figure 5) was lower than when based on more extensive sampling of jellyfish and zooplankton, which also incorporated sources of spatial and temporal variation.^{10,40} The use of GLS-tracked marine predator tissues to generate isoscapes could be improved by using these more complex models, such as Bayesian hierarchical integrated nested Laplace approximations (INLAs^{10,40}).

Studies of seabird isotopes geo-referenced by bird-borne GPS loggers reveal complexities which our study is less able to

characterise. For instance, $\delta^{13}\text{C}$ values of GPS-tracked Cory's shearwater (*Calonectris borealis*) plasma showed inshore-offshore and chlorophyll-driven variation in $\delta^{13}\text{C}$ values, whereas $\delta^{15}\text{N}$ values tended to vary temporally.³⁷ Moreover, long-term (17-year) feather isotope sampling of Cory's shearwaters revealed that both $\delta^{13}\text{C}$ and $\delta^{15}\text{N}$ values covaried with upwelling intensity in the CCLME.⁴¹ It might therefore be desirable to combine GPS and GLS-derived isotope values from multiple taxa to generate a more detailed picture of isotopic variability in space and time.

Our results using feathers from tracked gannets are like those based on fish muscle sampled at local ports across the southern portion of their wintering range (40° to 23° N; Figure 4). Although this

FIGURE 5 Interpolated isoscapes using empirical Bayesian kriging for (A,B) $\delta^{13}\text{C}$ and (C,D) $\delta^{15}\text{N}$ based on primary feathers of non-breeding gannets tracked with geolocators. Points are mean winter centroids, and black-surrounding lines represent 100 km radii illustrating approximate geolocation resolution. Blue boundary lines define large marine ecosystems [Color figure can be viewed at [wileyonlinelibrary.com](https://onlinelibrary.wiley.com)]



potential gannet prey was not sampled across the full wintering range of tracked birds, the direction and magnitude of isotopic gradients lend support to the efficacy of our combined GLS and feather isotope approach.²⁵

Large numbers of seabird species and individuals have now been tracked using geolocation around the world's oceans, providing detailed information about where and when birds are distributed.^{42–44} It might therefore be possible to create ocean basin-scale isoscapes using these data, retrospectively or strategically depending on whether there are extant feather samples or isotope measurements. Such an approach would also require a detailed reappraisal of seabird feather moult and over-winter site fidelity.

5 | CONCLUSIONS

To conclude, we demonstrate the efficacy of using geocator tracking of seabird migration and primary feather keratin to construct large-scale (thousands of kilometres) marine isoscapes. This was possible during non-breeding for a partially migratory species (and thus migratory destinations that vary latitudinally) at a time of the year when it is difficult to obtain higher-precision GPS tracking and contemporaneous blood sampling. Our confidence in the results is further improved through the incorporation of species-specific data on feather moult and isotopic measurements of potential prey across part of the gannet's wintering range. However, such an approach is likely to be less reliable at smaller spatial scales or where isotopic

gradients are less pronounced. We therefore urge continued study and refinement of these methods using more complex modelling in a range of different species and locations to continue to inform our knowledge of isotopic variation in marine ecosystems throughout annual cycles.

ACKNOWLEDGMENTS

The authors thank the following individuals for their generous contributions of photos used in their analysis of gannet moult: Alice Trevail, Murdo Messer, Beneharo Rodriguez, Catherine Jordan, Celia Ackerman, Charlotte Cummings, David Palmar, Enric Badosa, Jan Phillip, Geissel, Jessica Hey, Jo Anne Hood, Joseph Hames, Julien Gerngon, Kate Muir, Linda Scrima, Spea, Bianca P Vieira, Pedro Geraldes, Rita Matos, Nicola Hodgins, Nuno Oliveira, J. Gonin, Pep Arcos, Ron McIntyre, Rosie Brown, Steve Flynn, and Steve Truluck. The authors are grateful for the assistance of Ayoub Baali, Ahmed Yahyaoui, Sage Milestone, and numerous local fishermen during fieldwork conducted in Morocco. In addition, they thank Beth Clark, Liam Langley, Kirsty Laurenson, Aline Cerqueira, the RSPB, and Venture Jet for their hard work and logistical support during fieldwork conducted on Grassholm, Wales.

DATA AVAILABILITY STATEMENT

Data is available on request.

PEER REVIEW

The peer review history for this article is available at <https://publons.com/publon/10.1002/rcm.9489>.

ORCID

Stuart Bearhop  <https://orcid.org/0000-0002-5864-0129>

Thomas W. Bodey  <https://orcid.org/0000-0002-5334-9615>

W. James Grecian  <https://orcid.org/0000-0002-6428-719X>

Keith Hamer  <https://orcid.org/0000-0002-2158-2420>

Jason Newton  <https://orcid.org/0000-0001-7594-3693>

Richard B. Sherley  <https://orcid.org/0000-0001-7367-9315>

Stephen C. Votier  <https://orcid.org/0000-0002-0976-0167>

REFERENCES

- Hussey NE, Kessel ST, Aarestrup K, et al. Aquatic animal telemetry: A panoramic window into the underwater world. *Science*. 2015;348:1255-642.
- Kays R, Crofoot MC, Jetz W, Wikelski M. Terrestrial animal tracking as an eye on life and planet. *Science*. 2015;348:2478.
- Börger L, Bijleveld AI, Fayet AL, et al. Biologging special feature. *J Anim Ecol*. 2020;89:6-15.
- Chung H, Lee J, Lee WY. A review: Marine bio-logging of animal behaviour and ocean environments. *Ocean Sci J*. 2021;56(2):117-131. doi:10.1007/s12601-021-00015-1
- Fry B. *Stable Isotope Ecology*. New York: Springer; 2006.
- Phillips RA, Bearhop S, McGill RAR, Dawson DA. Stable isotopes reveal individual variation in migration strategies and habitat preferences in a suite of seabirds during the nonbreeding period. *Oecologia*. 2009;160:795-806.
- Inger R, Bearhop S. Applications of stable isotope analyses to avian ecology. *Ibis*. 2008;150:447-461.
- Ramos R, González-Solís J. Trace me if you can: The use of intrinsic biogeochemical markers in marine top predators. *Front Ecol Environ*. 2012;10:258-266.
- Carpenter-Kling T, Pistorius P, Reisinger R, Cherel Y, Connan M. A critical assessment of marine predator isoscapes within the southern Indian Ocean. *Mov Ecol*. 2020;8:1-18.
- St. John Glew K, Graham LJ, McGill RAR, Trueman CN. Spatial models of carbon, nitrogen and Sulphur stable isotope distributions (isoscapes) across a shelf sea: An INLA approach. *Methods Ecol Evol*. 2019;10:518-531.
- Magozzi S, Yool A, Vander Zanden HB, Wunder MB, Trueman CN. Using ocean models to predict spatial and temporal variation in marine carbon isotopes. *Ecosphere*. 2017;8:e01763.
- Trueman CN, MacKenzie KM, St John Glew K. Stable isotope-based location in a shelf sea setting: Accuracy and precision are comparable to light-based location methods. *Methods Ecol Evol*. 2017;8:232-240.
- Jaeger A, Lecomte VJ, Weimerskirch H, Richard P, Cherel Y. Seabird satellite tracking validates the use of latitudinal isoscapes to depict predators' foraging areas in the Southern Ocean. *Rapid Commun Mass Spectrom*. 2010;24:3456-3460.
- Phillips RA, Silk JRD, Croxall JP, Afanasyev V, Briggs DR. Accuracy of geolocation estimates for flying seabirds. *Mar Ecol Prog Ser*. 2004;266:265-272.
- Cherel Y, Quillfeldt P, Delord K, Weimerskirch H. Combination of at-sea activity, geolocation and feather stable isotopes documents where and when seabirds molt. *Front Ecol Evol*. 2016;4:3. doi:10.3389/fevo.2016.00003
- Fort J, Pettex E, Tremblay Y, et al. Meta-population evidence of oriented chain migration in northern gannets (*Morus bassanus*). *Front Ecol Environ*. 2012;10:237-242.
- Deakin Z, Hamer K, Sherley R, et al. Sex differences in migration and demography of a wide-ranging seabird, the northern gannet. *Mar Ecol Prog Ser*. 2019;622:191-201.
- Laurenson K, Atkins K, Clark BL, Morgan G, Morgan L, Votier SC. Gannet *Morus bassanus* ring recoveries suggest shorter migrations than geolocator tracking but indicate no long-term change in migration distances. *Bird Study*. 2021;68:1-8.
- Clark BL, Cox SL, Atkins KM, et al. Sexual segregation of gannet foraging over 11 years: Movements vary but isotopic differences remain stable. *Mar Ecol Prog Ser*. 2021;661:1-16.
- Nelson JB. *The Atlantic Gannet*. Great Yarmouth: Fenix Books; 2002.
- Griffiths R, Double MC, Orr K, Dawson RJG. A DNA test to sex most birds. *Mol Ecol*. 1998;7:1071-1075.
- Fridolfsson A-K, Ellegren H. A simple and universal method for molecular sexing of non-ratite birds. *J Avian Biol*. 1999;30:116.
- Stauss C, Bearhop S, Bodey TW, et al. Sex-specific foraging behaviour in northern gannets *Morus bassanus*: Incidence and implications. *Mar Ecol Prog Ser*. 2012;457:151-162.
- Osborne A, Ryan PG. Using digital photography to study moult extent in breeding seabirds. *Ostrich*. 2021;92(3):225-228.
- Meier RE, Votier SC, Wynn RB, et al. Tracking, feather moult and stable isotopes reveal foraging behaviour of a critically endangered seabird during the non-breeding season. *Divers Distrib*. 2017;23:130-145.
- Ginn H, Melville D. *Moult in birds*. London: BTO; 1983.
- Underhill LG, Zucchini W. A model for avian primary moult. *Ibis (Lond 1859)*. 1988;130:358-372.
- Erni B, Bonnevie BT, Oschadleus HD, Altwegg R, Underhill LG. Moult: An R package to analyze moult in birds. *J Stat Softw*. 2013;52:1-23.
- Grecian WJ, Williams HJ, Votier SC, et al. Individual spatial consistency and dietary flexibility in the migratory behavior of northern gannets wintering in the Northeast Atlantic. *Front Ecol Evol*. 2019;7:214. doi:10.3389/fevo.2019.00214
- Wotherspoon SJ, Sumner MD, Lisovski S. TwGeos: Basic data processing for light-level geolocation archival tags. 2016.

31. Rakhimberdiev E, Saveliev A, Piersma T, Karagicheva J. FLIGHTR: An R package for reconstructing animal paths from solar geolocation loggers. *Methods Ecol Evol.* 2017;8:1482-1487.
32. Votier SC, Bearhop S, Witt MJ, Inger R, Thompson D, Newton J. Individual responses of seabirds to commercial fisheries revealed using GPS tracking, stable isotopes and vessel monitoring systems. *J Appl Ecol.* 2010;47:487-497.
33. Marra G, Wood SN. Practical variable selection for generalized additive models. *Comput Stat Data Anal.* 2011;55:2372-2387.
34. Wood SN. Fast stable restricted maximum likelihood and marginal likelihood estimation of semiparametric generalized linear models. *J R Stat Soc Ser B (Statistical Methodol).* 2011;73:3-36.
35. R Core Team C. R: A language and environment for statistical computing. R Foundation for Statistical Computing; 2019.
36. Breiman L. Random forests. *Mach Learn.* 2001;45(1):5-32.
37. Ceia FR, Chérel Y, Paiva VH, Ramos JA. Stable isotope dynamics ($\delta^{13}\text{C}$ and $\delta^{15}\text{N}$) in neritic and oceanic waters of the North Atlantic inferred from GPS-tracked Cory's shearwaters. *Front Mar Sci.* 2018; 5:377.
38. Bates D, Mächler M, Bolker BM, Walker SC. Fitting linear mixed-effects models using lme4. *J Stat Softw.* 2014;67.
39. Sherman K. The large marine ecosystem concept: Research and management strategy for living marine resources. *Ecol Appl.* 1991;1: 349-360.
40. Espinasse B, Sturbois A, Basedow SL, et al. Temporal dynamics in zooplankton $\delta^{13}\text{C}$ and $\delta^{15}\text{N}$ isoscapes for the North Atlantic Ocean: Decadal cycles, seasonality, and implications for predator ecology. *Front Ecol Evol.* 2022;10:986082.
41. Ramos R, Reyes-González JM, Morera-Pujol V, Zajková Z, Militão T, González-Solís J. Disentangling environmental from individual factors in isotopic ecology: A 17-year longitudinal study in a long-lived seabird exploiting the canary current. *Ecol Indic.* 2020;111:105963.
42. Frederiksen M, Moe B, Daunt F, et al. Multicolony tracking reveals the winter distribution of a pelagic seabird on an ocean basin scale. *Divers Distrib.* 2012;18:530-542.
43. Grecian WJ, Witt MJ, Attrill MJ, et al. Seabird diversity hotspot linked to ocean productivity in the canary current large marine ecosystem. *Biol Lett.* 2016;12:20160024.
44. Davies TE, Carneiro APB, Tarzia M, et al. Multispecies tracking reveals a major seabird hotspot in the North Atlantic. *Conserv Lett.* 2021;14:e12824.

SUPPORTING INFORMATION

Additional supporting information can be found online in the Supporting Information section at the end of this article.

How to cite this article: Atkins K, Bearhop S, Bodey TW, et al. Geolocator-tracking seabird migration and moult reveal large-scale, temperature-driven isoscapes in the NE Atlantic. *Rapid Commun Mass Spectrom.* 2023;37(9):e9489. doi:[10.1002/rcm.9489](https://doi.org/10.1002/rcm.9489)